JOURNAL OF VIROLOGY, May 1996, p. 3242–3247 Vol. 70, No. 5
0022-538X/96/$04.00+0

NOTES

Subcellular Localization of Aleutian Mink Disease Parvovirus Proteins and DNA during Permissive Infection of Crandell Feline Kidney Cells

MARTIN B. OLEKSIEWICZ,[1] FRED COSTELLO,[1] MARK HUHTANEN,[1] JAMES B. WOLFINBARGER,[1] SOREN ALEXANDERSEN,[2] AND MARSHALL E. BLOOM[1]*

Laboratory of Persistent Viral Diseases, Rocky Mountain Laboratories, National Institute of Allergy and Infectious Diseases, Hamilton, Montana 59840,[1] and Danish Veterinary Institute for Virus Research, Lindholm, DK-4771 Kalvehave, Denmark[2]

Received 7 December 1995/Accepted 7 February 1996

Confocal microscopy allowed us to localize viral nonstructural (NS) and capsid (VP) proteins and DNA simultaneously in cells permissively infected with Aleutian mink disease parvovirus (ADV). Early after infection, NS proteins colocalized with viral DNA to form intranuclear inclusions, whereas VP proteins formed hollow intranuclear shells around the inclusions. Later, nuclei had irregular outlines and were virtually free of ADV products. In these cells, inclusions of viral DNA with or without associated NS protein were embedded in cytoplasmic VP protein. These findings implied that ADV replication within an infected cell is regulated spatially as well as temporally.

A close correlation exists between the pathogenesis of disease induced by the Aleutian mink disease parvovirus (ADV) and viral replication at the single-cell level. Acute ADV infection of type II pneumocytes in mink kits is permissive and leads to a fulminant pneumonia (3, 4, 9, 27). Chronic infection of adult mink, on the other hand, is associated with profound immune disturbances and restricted viral replication in lymphoid tissues (2, 4, 9, 20–22).

Parvovirus replication is an intranuclear process dependent on cell cycle and cellular differentiation (16). During replication, the single-stranded DNA genome is converted to duplex replicative intermediates that function as templates for genomic amplification and transcription as well as a source for progeny single-stranded genomes (16). The 4,800-base single-stranded ADV genome codes for at least two nonstructural (NS) proteins (NS1 and NS2) and two capsid (VP) proteins (VP1 and VP2) (1, 7–9, 12, 13, 42). Viral DNA replication and efficient viral transcription require the pleiotropic NS1 protein (11, 33, 34, 39). The smaller, NS2 protein regulates the production of viral proteins (23, 24, 28). For ADV, minus-sense single-stranded progeny genomes are packaged in 25-nm icosahedral capsids consisting of VP1 and VP2 in a 1/10 ratio (16).

Intracellular compartmentalization of viral products may be a higher-order regulatory mechanism for viruses, including parvoviruses (37, 40, 44). For example, coinfection with adenovirus type 2 facilitates replication of the parvovirus minute virus of mice in HeLa cells, and this is associated with the shifting of minute virus of mice DNA to replication factories in the peripheral nuclear matrix (26). In addition, permissive replication of parvovirus H-1 depends on effective nuclear transport of NS1 in certain cell types (35). Thus, the precise cellular location of viral components might influence the outcome of parvovirus infection.

Several previous publications have described the distribution of ADV proteins and nucleic acids within infected cells (3, 27); however, no information exists on how the two classes (NS and VP) of ADV proteins colocalize with viral DNA in situ during permissive or restricted infection. To provide a framework for comparison, we used confocal microscopy to examine the localization of ADV proteins and DNA during permissive infection.

For the detection of NS proteins, ADV segments specific for NS1 (ADV-G nucleotides 722 to 1596) (1, 8) and NS2 (ADV-G nucleotides 2043 to 2210) (1, 8) were expressed as fusion proteins in frame with the maltose-binding protein in pMAL-c2 (New England Biolabs, Beverly, Mass.) (5, 19, 25, 43). Maltose-binding protein–ADV fusion proteins were purified by affinity chromatography on amylose resin columns (25) and used to immunize rabbits. The rabbit anti-NS immunoglobulin G (27, 31) was conjugated to fluorescein isothiocyanate. A cocktail of murine monoclonal antibodies reactive against both VP1 and VP2 was used to detect ADV VP proteins (32). DNA probes for the detection of ADV DNA were prepared by PCR (29). Four different ADV DNA fragments of 220 to 240 bp in length, spanning 20 to 68 map units (1, 8), were labeled in standard PCR mixtures (29) containing 200 μM Cy-5 dCTP (Molecular Probes, Eugene, Oreg.), pooled, purified on spin filters, and stored at 5 to 10 ng/μl at −20°C.

A triple stain for ADV NS proteins, VP proteins, and DNA was performed on monolayers in slide chambers. For fluorescent in situ hybridization, previously used protocols were modified (3). Slides were incubated in 10 mM Tris (pH 7.4)–15 mM NaCl–200 μg of DNase-free RNase I (Pharmacia) per ml for 15 min at 37°C and then prehybridized for 30 min at 50°C in hybridization solution (50% formamide–5× SSC [1× SSC is 0.15 M NaCl plus 0.015 M sodium citrate]–0.5% sodium dodecyl sulfate [SDS]–500 μg of denatured salmon sperm DNA

* Corresponding author. Mailing address: Laboratory of Persistent Viral Diseases, Rocky Mountain Laboratories, Hamilton, MT 59840. Phone: (406) 363-9275. Fax: (406) 363-9204. Electronic mail address: mbloom@nih.gov.

FIG. 1. Colocalization of ADV DNA, NS proteins, and VP proteins. ADV-infected asynchronous CRFK cultures were harvested 3 days postinfection and triple stained as described in the text. Representative confocal optical sections through the nucleus of a single infected cell are shown. The staining patterns for ADV NS proteins, DNA, and VP proteins (a, b, and c, respectively) are shown separately in black and white and are merged in color (d; NS proteins in green, DNA in blue, and VP proteins in red, colocalizing NS protein-DNA appears as turquoise, NS protein-VP protein appears as yellow, and DNA-VP protein appears as violet. Bar, 10 μm. See text for discussion.

per ml). After denaturation for 20 min at 65°C in 95% formamide–0.1× SSC, slides were hybridized for 2 h at 50°C with 200 to 400 ng of heat-denatured ADV probe per ml. Next, slides were washed twice at 65°C in 0.1× SSPE (1× SSPE is 0.18 M NaCl, 10 mM NaH_2PO_4, and 1 mM EDTA [pH 7.7])–0.1% SDS. For subsequent staining for ADV proteins, slides were blocked and incubated for 1 h at room temperature in a cocktail of the fluorescein isothiocyanate-conjugated anti-NS rabbit immunoglobulin G and the three monoclonal antibodies (MAbs). After a 5-min wash in phosphate-buffered saline (PBS)–0.5% Tween 20, slides were incubated for 30 to 45 min in a 1:200 dilution of rhodamine-conjugated goat anti-mouse immunoglobulin, washed in PBS–0.5% Tween 20, and mounted in an anti-fade mounting medium. Negative controls for the triple stain procedure included uninfected Crandell feline kidney (CRFK) cells, CRFK cells infected with another parvovirus, mink enteritis virus, and omission of the MAbs against ADV VP proteins.

VP proteins were also localized in CRFK cells that had been fixed in 3.5% paraformaldehyde in PBS for 10 min, permeab-

FIG. 2. Subcellular localization of ADV VP proteins. ADV-infected asynchronous CRFK cultures were harvested 3 days postinfection, fixed in paraformaldehyde, and stained with an anti-VP MAb cocktail and propidium iodide. Single confocal optical sections through infected cells are shown. ADV VP proteins are shown in green, the signal from propidium iodide is shown in red, and overlap is shown in yellow. (a) Early-infection cells; (b) late-infection cell. Bars, 10 μm. See text for discussion.

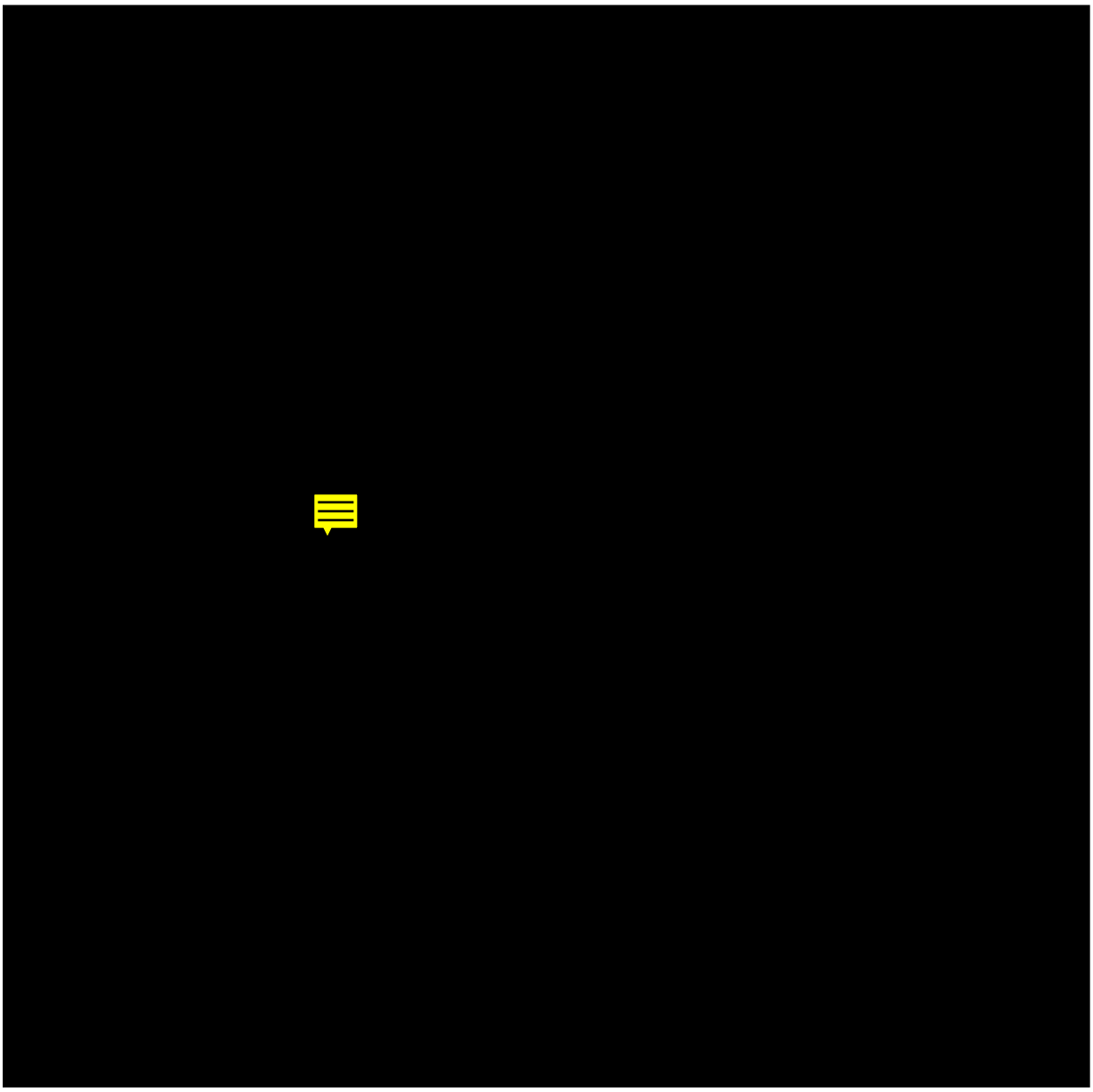

FIG. 3. Colocalization of ADV DNA, NS proteins, and VP proteins in synchronized cells. Synchronized CRFK cultures infected with ADV and harvested at 45 (a to e) or 75 (f to j) h postrelease were triple stained and examined by confocal microscopy. Shown are single confocal optical sections through groups of infected cells. The magnification, field of view, and confocal sectioning depth are the same in panels a through e and panels f through j. Bars, 10 μm. Fluorescent signals from NS protein (c and h), DNA (d and j), and VP protein (e and i) stains are shown separately in black and white and merged in color (a and f), as described in the legend to Fig. 1. (b and g) Phase-contrast pictures. See text for discussion.

ilized for 3 min in 0.1% Triton X in PBS, and stained with the MAb anti-VP cocktail. These slides were counterstained with 1 μg of propidium iodide per ml–200 μg of RNase per ml in PBS to visualize cell nuclei in the absence of fluorescent in situ hybridization.

Confocal microscopy was performed with a Zeiss Axiovert inverted microscope fitted with a Bio-Rad MRC 1000 laser confocal module (6). There was no spectral overlap among the three fluorochromes (6). Digitalized images from each of the three fluorochromes in a representative optical section through infected cells were initially acquired by using Comos software. Three-color images were generated by using Confocal Assistant (Bio-Rad) and Adobe Photo Workshop (Adobe Systems, Inc., Mountain View, Calif.).

Asynchronous CRFK cells were infected with 20 fluorescence-forming units of ADV-G per cell (10). At the indicated times monolayers were fixed in acetone. Some cultures were synchronized in early S phase by a double-block regimen of topoinhibition and hydroxyurea treatment (18). Topoinhibited cells were infected with 20 fluorescence-forming units of ADV-G per cell in media containing 0.002 M hydroxyurea and incubated at 37°C until release from the block. They were then incubated at 31.8°C. A detailed description will be given elsewhere (30).

In asynchronous CRFK cultures studied 2 to 3 days postinfection, a characteristic cell morphology was observed. In these cells, the bulk of ADV DNA colocalized with NS proteins in intranuclear inclusions (Fig. 1; compare panel a [NS] with

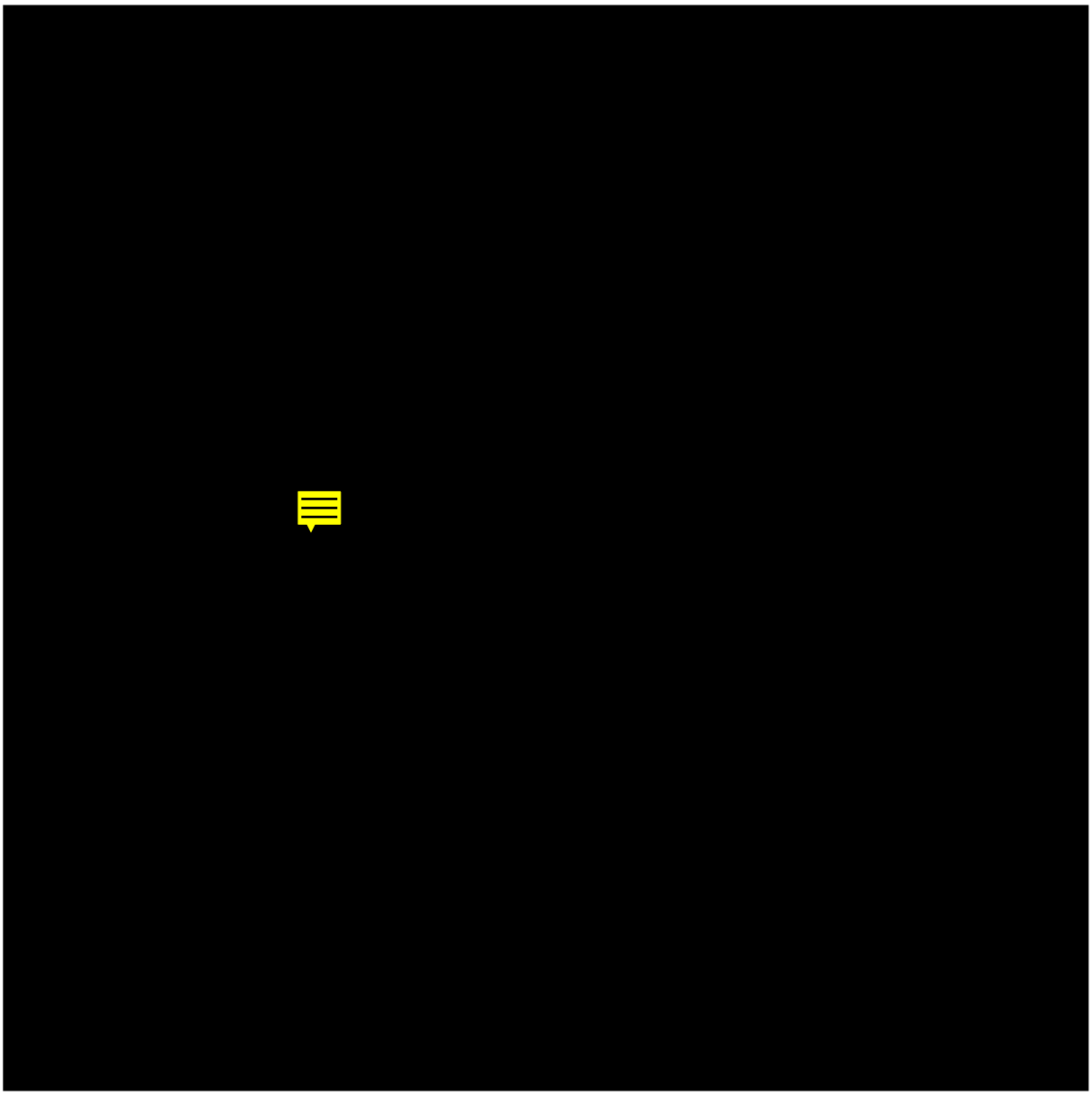

FIG. 3—*Continued.*

panel b [DNA]). Note the almost exact colocalization in every limb of this complex honeycombed structure. The nuclear localization of NS protein-viral DNA inclusions was obvious in phase-contrast pictures (see below). The complex three-dimensional structure of the inclusions, when examined by confocal z-sectioning (6), ranged from solid to honeycombed, and the size varied from being small to encompassing virtually the whole of the infected nucleus.

VP proteins in these cells were concentrated in shell-like structures surrounding the intranuclear NS protein-viral DNA inclusions. In a single optical section (Fig. 1c), the VP proteins appear as a ring, but confocal z-sectioning confirmed the three-dimensional structure. There was little overlap (shown in yellow) evident between VP protein shells and NS protein-viral DNA inclusions (Fig. 1d). The subcellular localization of the VP shells was identical (yellow rings in Fig. 2a) in paraformaldehyde-fixed cells in which the nuclei had been counterstained with propidium iodide, showing that the shells were not procedural artifacts. In single confocal sections, VP shells showed complete overlap with the propidium iodide signal, indicating that VP shells were confined within the nucleus, closely opposed to the nuclear border. Nuclei containing VP shells typically had sharp outlines similar to those of uninfected interphase nuclei.

An alternative morphology, with VP proteins localized exclusively in the cytoplasm, was also observed (Fig. 2b). These cells had nuclei with irregular outlines, and small granules of DNA were dispersed throughout the cytoplasm (Fig. 2b; DNA granules are shown in red or yellow, depending on the degree of overlap with VP proteins; the arrow points to a large DNA granule; numerous other granules are present in the cytoplasm). The nuclei of such cells were remarkably empty of VP proteins (Fig. 2b; the nucleus is shown in red, and any intranuclear VP protein would be shown in yellow). This morphology

suggested an end stage in infection, at which ADV-mediated cytotoxic injury had compromised nuclear integrity and led to the release of viral products to the cytoplasm.

In synchronized CRFK cultures, no specific ADV signal was observed until 6 h after hydroxyurea release, confirming that replication is dependent on the cellular S phase (16). By 6 to 8 h postrelease, ADV DNA and NS and VP proteins were noted in small, weakly staining intranuclear foci (not shown), but the signal was poorly resolved and present only in a small number of cells.

Between 12 and 45 h postrelease, the signal from ADV DNA and proteins became strong. Many cells exhibited the layered arrangement of VP shells around intranuclear inclusions of NS protein and viral DNA (Fig. 3a; arrow) described above. Minor variations of this morphology, for example, at points (Fig. 3a; arrowhead) where the overlap between NS and VP proteins was larger, were also noted. Phase-contrast examination clearly demonstrated that the localization of the NS protein-viral DNA inclusions was nuclear (Fig. 3; compare panels a and b; the arrow in panel b points to the nuclear border).

Later than 72 h after release, both VP proteins as well as the NS protein-viral DNA complexes localized to the cytoplasm (Fig. 3; compare panel h [NS] with panel j [DNA]; colocalizing NS proteins and viral DNA are shown in panel f in turquoise or yellow [overlap with VP proteins]; viral DNA without associated NS proteins is shown in blue or violet [overlap with VP proteins]). The nuclei at that time were remarkably devoid of viral proteins and DNA (Fig. 3f; arrow; compare with the cell just below, in which the nucleus still contains some NS proteins and viral DNA).

Taken together, our results suggested that the distribution patterns of viral DNA and proteins shown in Fig. 1 to 3 reflect a time-dependent sequence of viral replication and cytotoxic injury. For convenience, the patterns can be grouped in two main categories: (i) early infection, when NS proteins and viral DNA colocalized in intact nuclei (Fig. 1d, 2a, and 3a); and (ii) late infection, when colocalizing NS proteins and viral DNA were found as small cytoplasmic granules in cells with damaged nuclei (Fig. 2b and 3f). In both categories, VP proteins overlapped with the spherical NS protein-viral DNA complexes only at their margins. VP proteins were found either in intranuclear shell-like structures in early infection (Fig. 2a) or in the cytoplasm in late infection (Fig. 2b). Consequently, two new findings emerged from these studies. First, NS proteins colocalized with viral DNA as inclusions in the nuclei of infected cells (Fig. 1). Second, VP proteins within the nucleus were present in shell-like structures near the nuclear margin and were largely excluded from the NS protein-viral DNA inclusions (Fig. 1d).

Although both ADV DNA and NS proteins are known to localize in the nucleus, we demonstrated a close spatial association between parvoviral DNA and NS proteins in infected cells in situ (Fig. 1; compare panel a [NS] with panel b [DNA]). This result is striking but perhaps not surprising, as NS proteins function in parvoviral DNA replication and gene expression and NS1 binds specifically to viral DNA in vitro (15). The size and staining intensity of the inclusions increased from 6 to 12 h postrelease in synchronized cells. Therefore, we assume that inclusions of the type shown in Fig. 1d and 3a (colocalizing NS proteins and viral DNA shown in turquoise) contain actively replicating ADV DNA. Experiments with monospecific reagents are planned to directly address the question of whether ADV NS1 and NS2 have differential localization in relation to each other, VP proteins, and viral DNA.

The intranuclear shells of VP were not resolved in previous studies in which the same anti-VP MAbs were used for immunofluorescence analysis (3, 32). The hollow shell structures that are so striking in single confocal optical sections appear more as solid bodies when viewed by epifluorescence.

It is uncertain at present if the striking peripheral concentration of VP seen early after infection has any functional importance (Fig. 2a). In this regard, expression of the minute virus of mice VP protein has been shown to be toxic to murine cells (14) and perhaps the intranuclear VP shells somehow contribute to parvoviral cytotoxicity. Alternatively, topographical segregation of replicating viral DNA and NS proteins from the VP shells might also regulate interactions between replicative intermediates. In contrast, in late-infection cells, we observed fragmentation of the intranuclear inclusions and cytoplasmic colocalization of VP proteins and NS protein-viral DNA complexes (3, 27, 36). NS proteins are important for encapsidation and maturation (17, 23), and there is also a precedent for differential processing of parvoviral DNA in the presence or absence of VP proteins (17, 23). However, it is unclear if our observations are the morphological manifestations of these biochemical findings.

Another important question is the relationship of the intranuclear VP protein shells (Fig. 2a) to capsids. Interestingly, concentration of unassembled capsid protein was observed in marginated heterochromatin along the border of H-1-infected nuclei, whereas both empty and full H-1 capsids were distributed diffusely throughout the nucleus (38). However, whether the empty capsids commonly observed in infected nuclei serve as precursors for full capsids or whether full and empty capsids arise from unassembled capsid proteins by parallel pathways remains undetermined (38, 41).

In conclusion, we have described permissive ADV replication in terms of the precise subcellular colocalization of viral NS proteins, VP proteins, and DNA. Work is currently under way to further refine the localization of ADV products in CRFK cells by triple-label immunofluorescence with antibodies monospecific for NS1, NS2, and VP1. Finally, we plan to determine whether these localization patterns are altered during restricted ADV infection, as occurs in macrophages (21).

We thank Lucia Barker for an expert introduction to the field of confocal microscopy, Robert Evans and Gary Hettrick for artwork, and Katrina Oie for help with PCR. Stanley Falkow, Torben Storgaard, and Linda Dworak participated in helpful discussions.

M.B.O. was an NIH Special Volunteer, employed by the Department of Pharmacology and Pathobiology, The Royal Veterinary and Agricultural University, Copenhagen, Denmark, and partly supported by grant S950008 from The Danish Research Academy.

REFERENCES

1. **Alexandersen, S., M. E. Bloom, and S. Perryman.** 1988. Detailed transcription map of Aleutian mink disease parvovirus. J. Virol. **62:**3684–3694.
2. **Alexandersen, S., M. E. Bloom, and J. Wolfinbarger.** 1988. Evidence of restricted viral replication in adult mink infected with Aleutian disease of mink parvovirus. J. Virol. **62:**1495–1507.
3. **Alexandersen, S., M. E. Bloom, J. Wolfinbarger, and R. E. Race.** 1987. In situ molecular hybridization for detection of Aleutian mink disease parvovirus DNA by using strand-specific probes: identification of target cells for viral replication in cell cultures and in mink kits with virus-induced interstitial pneumonia. J. Virol. **61:**2407–2419.
4. **Alexandersen, S., T. Storgaard, N. Kamstrup, B. Aasted, and D. D. Porter.** 1994. Pathogenesis of Aleutian mink disease parvovirus infection: effects of suppression of antibody response on viral mRNA levels and on development of acute disease. J. Virol. **68:**738–749.
5. **Amman, E., J. Brosius, and M. Ptashne.** 1983. Vectors bearing a hybrid trp-lac promoter useful for regulated expression of cloned genes in Escherichia coli. Gene **25:**167–188.
6. **Bio-Rad Laboratories, Inc.** 1994. MRC-1000 operating manual. Bio-Rad Microscience, Ltd., Hercules, Calif.

7. **Bloom, M. E., S. Alexandersen, C. F. Garon, S. Mori, W. Wei, S. Perryman, and J. B. Wolfinbarger.** 1990. Nucleotide sequence of the 5′-terminal palindrome of Aleutian mink disease parvovirus and construction of an infectious molecular clone. J. Virol. **64:**3551–3556.
8. **Bloom, M. E., S. Alexandersen, S. Perryman, D. Lechner, and J. B. Wolfinbarger.** 1988. Nucleotide sequence and genomic organization of Aleutian mink disease parvovirus (ADV): sequence comparisons between a nonpathogenic and a pathogenic strain of ADV. J. Virol. **62:**2903–2915.
9. **Bloom, M. E., H. Kanno, S. Mori, and J. B. Wolfinbarger.** 1994. Aleutian mink disease: puzzles and paradigms. Infect. Agents Dis. **3:**279–301.
10. **Bloom, M. E., R. E. Race, and J. B. Wolfinbarger.** 1980. Characterization of Aleutian disease virus as a parvovirus. J. Virol. **35:**836–843.
11. **Christensen, J., M. Pedersen, B. Aasted, and S. Alexandersen.** 1995. Purification and characterization of the major nonstructural protein (NS-1) of Aleutian mink disease parvovirus. J. Virol. **69:**1802–1809.
12. **Christensen, J., T. Storgaard, B. Bloch, S. Alexandersen, and B. Aasted.** 1993. Expression of Aleutian mink disease parvovirus proteins in a baculovirus vector system. J. Virol. **67:**229–238.
13. **Clemens, D. L., J. B. Wolfinbarger, S. Mori, B. D. Berry, S. F. Hayes, and M. E. Bloom.** 1992. Expression of Aleutian mink disease parvovirus capsid proteins by a recombinant vaccinia virus: self-assembly of capsid proteins into particles. J. Virol. **66:**3077–3085.
14. **Clemens, K. E., D. R. Cerutis, L. R. Burger, C. Q. Yang, and D. J. Pintel.** 1990. Cloning of minute virus of mice cDNAs and preliminary analysis of individual viral proteins expressed in murine cells. J. Virol. **64:**3967–3973.
15. **Cotmore, S. F., J. Christensen, J. P. F. Nüesch, and P. Tattersall.** 1995. The NS1 polypeptide of the murine parvovirus minute virus of mice binds to DNA sequences containing the motif $[ACCA]_{2-3}$. J. Virol. **69:**1652–1660.
16. **Cotmore, S. F., and P. Tattersall.** 1987. The autonomously replicating parvoviruses. Adv. Virus Res. **33:**91–174.
17. **Cotmore, S. F., and P. Tattersall.** 1989. A genome-linked copy of the NS-1 polypeptide is located on the outside of infectious parvovirus particles. J. Virol. **63:**3902–3911.
18. **Fantes, P., and R. Brooks.** 1993. The cell cycle: a practical approach. IRL Press, Oxford.
19. **Guan, C., P. Li, P. D. Riggs, and H. Inouye.** 1987. Vectors that facilitate the expression and purification of foreign peptides in *Escherichia coli* by fusion to maltose binding protein. Gene **67:**21–30.
20. **Kanno, H., J. B. Wolfinbarger, and M. E. Bloom.** 1992. Identification of Aleutian mink disease parvovirus transcripts in macrophages of infected adult mink. J. Virol. **66:**5305–5312.
21. **Kanno, H., J. B. Wolfinbarger, and M. E. Bloom.** 1993. Aleutian mink disease parvovirus infection of mink macrophages and human macrophage cell line U937: demonstration of antibody-dependent enhancement of infection. J. Virol. **67:**7017–7024.
22. **Kanno, H., J. B. Wolfinbarger, and M. E. Bloom.** 1993. Aleutian mink disease parvovirus infection of mink peritoneal macrophages and human macrophage cell lines. J. Virol. **67:**2075–2082.
23. **Li, X., and S. L. Rhode III.** 1991. Nonstructural protein NS2 of parvovirus H-1 is required for efficient viral protein synthesis and virus production in rat cells in vivo and in vitro. Virology **184:**117–130.
24. **Li, X., and S. L. Rhode III.** 1993. The parvovirus H-1 NS2 protein affects viral gene expression through sequences in the 3′ untranslated region. Virology **194:**10–19.
25. **Maina, C., P. D. Riggs, A. G. Grandea III, B. E. Slatko, L. S. Moran, J. A. Tagliante, L. A. McReynolds, and C. di Guan.** 1988. An Escherichia coli vector to express and purify foreign proteins by fusion to and separation from maltose-binding protein. Gene **74:**365–373.
26. **Moen, P. T., Jr., E. Fox, and J. W. Bodnar.** 1990. Adenovirus and minute virus of mice DNAs are localized at the nuclear periphery. Nucleic Acids Res. **18:**513–521.
27. **Mori, S., J. B. Wolfinbarger, N. Dowling, W. Wei, and M. E. Bloom.** 1991. Simultaneous identification of viral proteins and nucleic acids in cells infected with Aleutian mink disease parvovirus. Microb. Pathog. **9:**243–253.
28. **Naeger, L. K., N. Salomé, and D. J. Pintel.** 1993. NS2 is required for efficient translation of viral mRNA in minute virus of mice-infected murine cells. J. Virol. **67:**1034–1043.
29. **Oie, K. L., G. Durrant, J. B. Wolfinbarger, D. Martin, F. Costello, S. Perryman, D. Hogan, W. J. Hadlow, and M. E. Bloom.** 1996. The relationship between capsid protein (VP2) sequence and pathogenicity of Aleutian mink disease parvovirus (ADV): a possible role for raccoons in the transmission of ADV infections. J. Virol. **70:**852–861.
30. **Oleksiewicz, M. B.** Unpublished data.
31. **Porter, D. D., H. G. Porter, and A. E. Larsen.** 1990. Aleutian disease parvovirus infection of mink and ferrets elicits an antibody response to a second nonstructural viral protein. J. Virol. **64:**1859–1860.
32. **Race, R. E., B. Chesebro, M. E. Bloom, B. Aasted, and J. Wolfinbarger.** 1986. Monoclonal antibodies against Aleutian disease virus distinguish virus strains and differentiate sites of virus replication from sites of viral antigen sequestration. J. Virol. **57:**285–293.
33. **Rhode, S. L., III.** 1985. *trans*-activation of parvovirus P_{38} promoter by the 76K noncapsid protein. J. Virol. **55:**886–889.
34. **Rhode, S. L., III.** 1989. Both excision and replication of cloned autonomous parvovirus DNA require the NS1 (*rep*) protein. J. Virol. **63:**4249–4256.
35. **Rhode, S. L., III, and P. R. Paradiso.** 1989. Parvovirus replication in normal and transformed human cells correlates with nuclear translocation of the early protein NS1. J. Virol. **63:**349–355.
36. **Richards, R., P. Linser, and R. Armentrout.** 1977. Kinetics of assembly of a parvovirus, minute virus of mice, in synchronized rat brain cells. J. Virol. **22:** 778–793.
37. **Schirmbeck, R., and W. Deppert.** 1989. Nuclear subcompartmentalization of simian virus 40 large T antigen: evidence for in vivo regulation of biochemical activities. J. Virol. **63:**2308–2316.
38. **Singer, I. I., and S. L. Rhode III.** 1978. Electron microscopy and cytochemistry of H-1 parvovirus intracellular morphogenesis, p. 479–504. *In* D. C. Ward and P. Tattersall (ed.), Replication of mammalian parvoviruses. Cold Spring Harbor Press, New York.
39. **Van Hille, B., N. Duponchel, N. Salome, N. Spruyt, S. F. Cotmore, P. Tattersall, J. J. Cornelis, and J. Rommelaere.** 1989. Limitations to the expression of parvoviral nonstructural proteins may determine the extent of sensitization of EJ-ras-transformed rat cells to minute virus of mice. Virology **171:**89–97.
40. **Voelkerding, K., and D. F. Klessig.** 1986. Identification of two nuclear subclasses of the adenovirus type 5-encoded DNA-binding protein. J. Virol. **60:** 353–362.
41. **Wistuba, A., S. Weger, A. Kern, and J. A. Kleinschmidt.** 1995. Intermediates of adeno-associated virus type 2 assembly: identification of soluble complexes containing Rep and Cap proteins. J. Virol. **69:**5311–5319.
42. **Wu, W.-H., M. E. Bloom, B. D. Berry, M. J. McGinley, and K. B. Platt.** 1994. Expression of Aleutian mink disease parvovirus capsid proteins in a baculovirus expression system for potential diagnostic use. J. Vet. Diagn. Invest. **6:**23–29.
43. **Yanisch-Perron, C., J. Vieira, and J. Messing.** 1985. Improved M13 phage cloning vectors and host strains: nucleotide sequences of the M13mp18 and pUC19 vectors. Gene **33:**103–119.
44. **Zhu, Z., W. Cai, and P. A. Schaffer.** 1994. Cooperativity among herpes simplex virus type 1 immediate-early regulatory proteins: ICP4 and ICP27 affect the intracellular localization of ICP0. J. Virol. **68:**3027–3040.

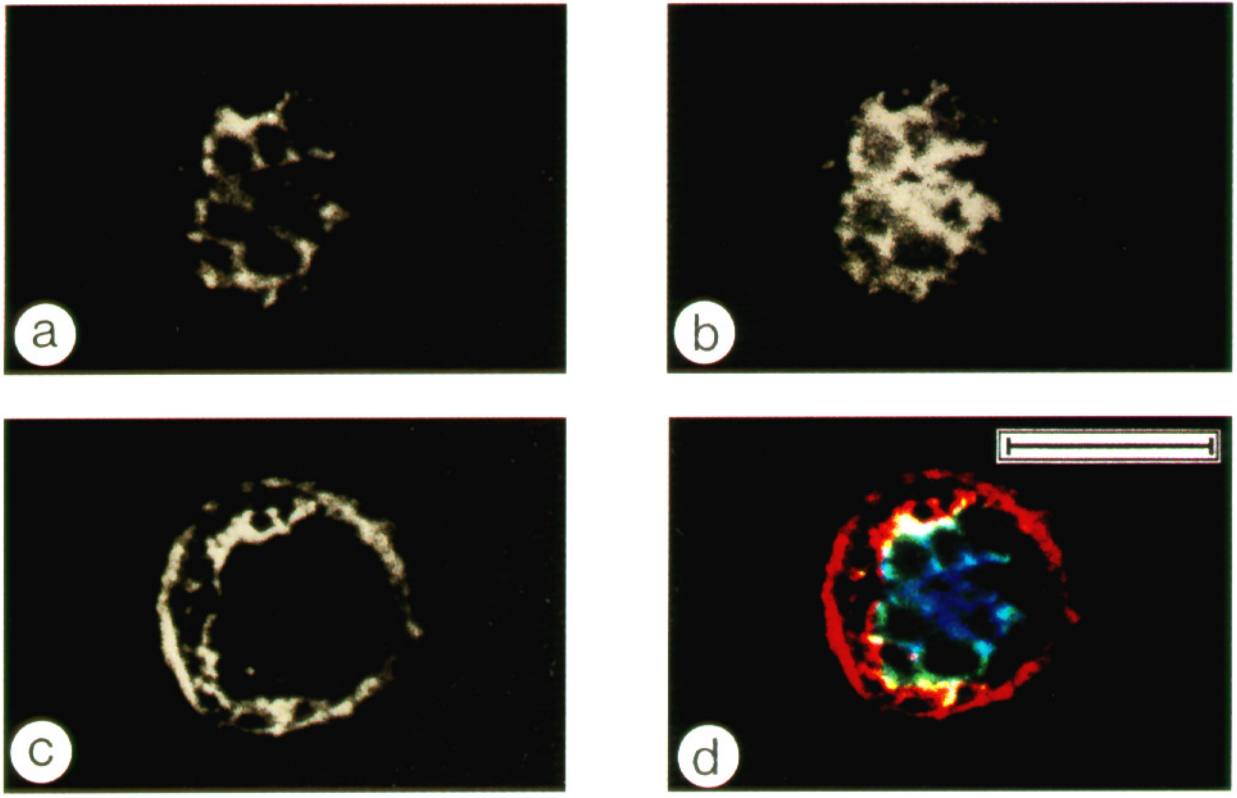
a
b
c
d

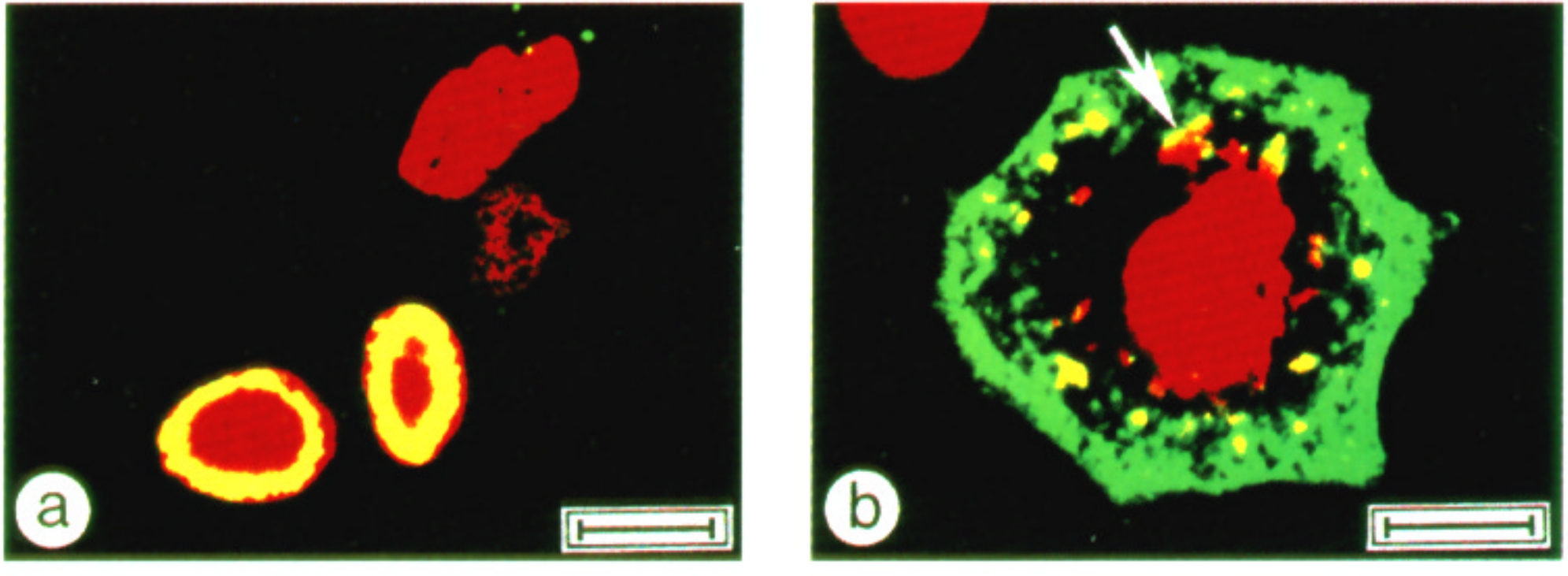
a
b

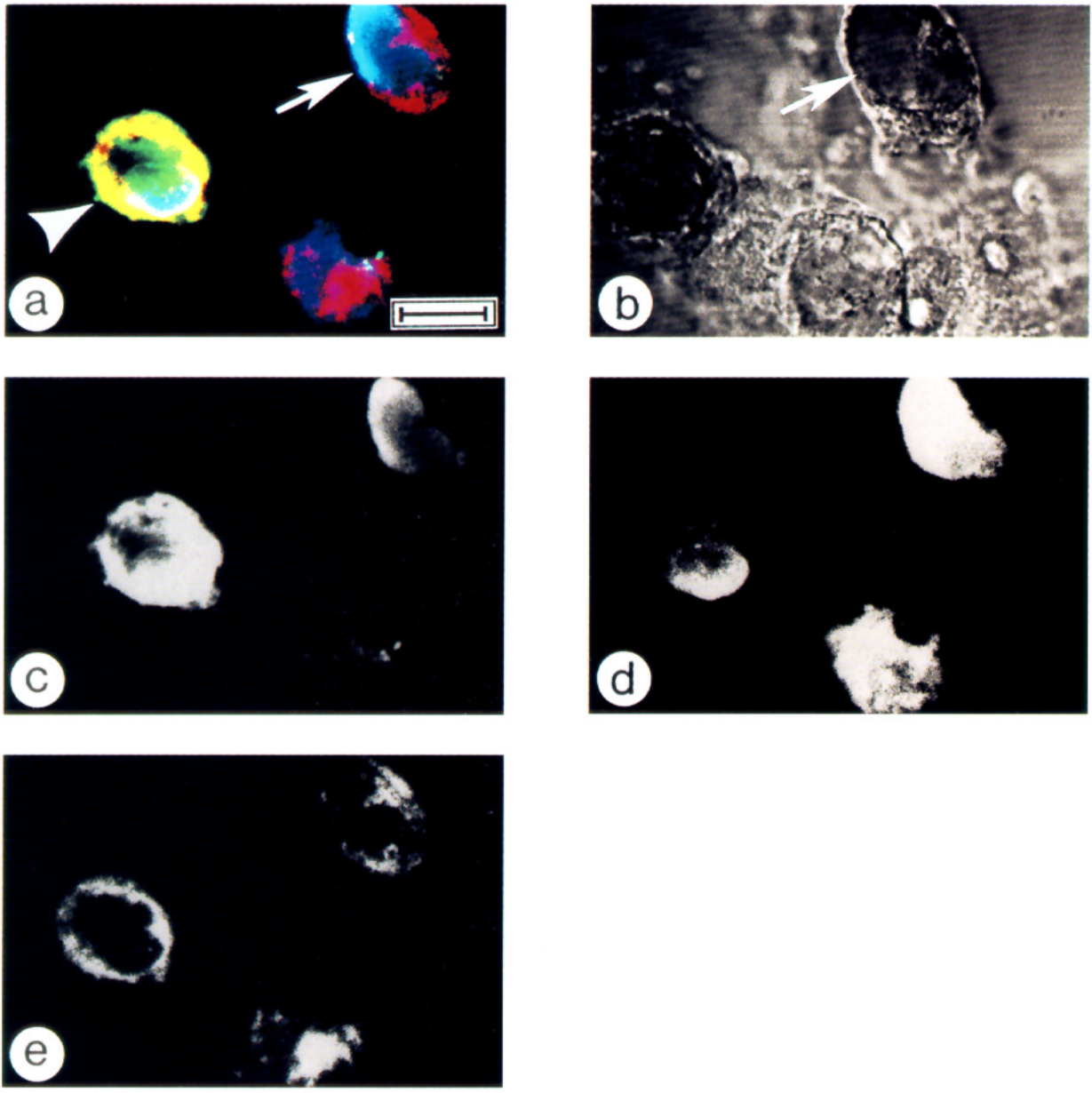
a
b
c
d
e

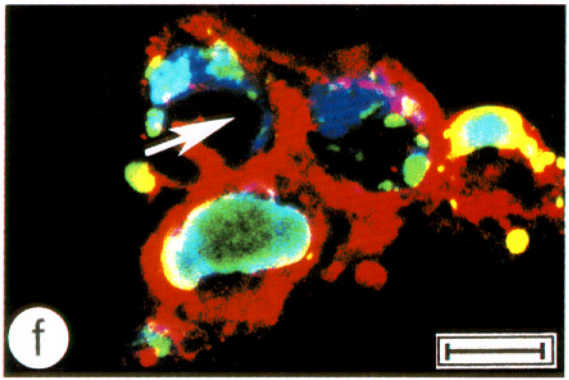
f

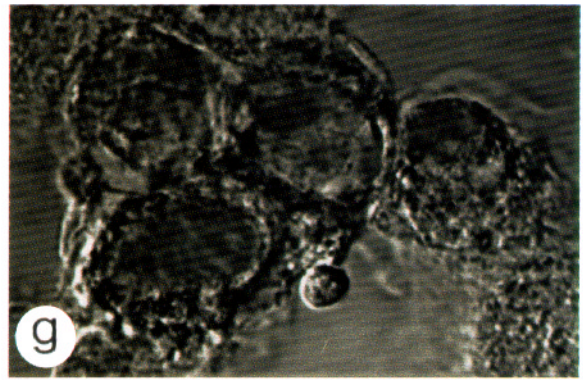
g

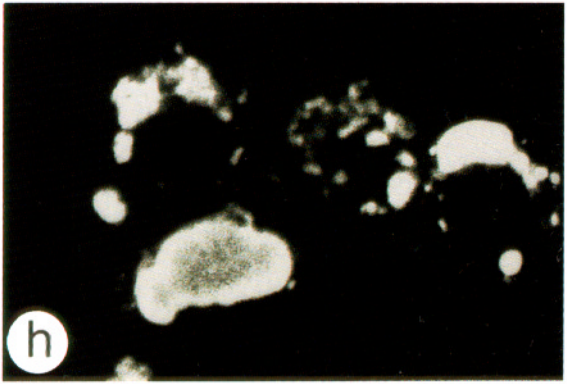
h

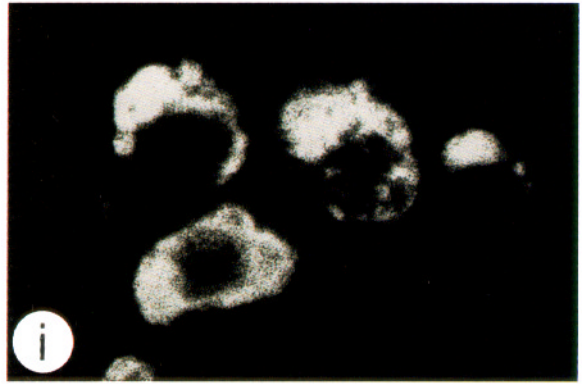
i

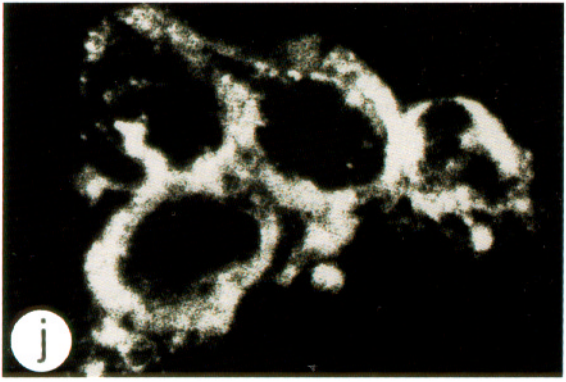
j